

Environmental Effects on Phosphoryl Group Bonding Probed by Vibrational Spectroscopy: Implications for Understanding Phosphoryl Transfer and Enzymatic Catalysis

Hu Cheng,^{†,||} Ivana Nikolic-Hughes,[#] Jianghua H. Wang,^{†,⊥} Hua Deng,[†]
Patrick J. O'Brien,^{†,⊕} Li Wu,[‡] Zhong-Yin Zhang,[‡] Daniel Herschlag,^{*,#,†,§} and
Robert Callender^{*,†}

Contribution from the Department of Biochemistry, Albert Einstein College of Medicine, Bronx, New York 10461-1602, Department of Chemical Engineering, Stanford University, Stanford, California 94305-5025, Department of Biochemistry, Stanford University, Stanford, California 94305-5307, Department of Molecular Pharmacology, Albert Einstein College of Medicine, Bronx, New York 10461-1602, and Department of Chemistry, Stanford University, Stanford, California 94305-5080

Received April 10, 2002

Abstract: We have used vibrational spectroscopy to study bonding in monosubstituted dianionic phosphates, both to learn more about basic properties intrinsic to this important class of biological substrates and to assess the ability of vibrational spectroscopy to provide a “sensor” or probe of the local environment experienced by the phosphoryl group. We examined the bonding properties of the phosphoryl group via vibrational spectroscopy for a series of compounds in which the phosphoryl substituent was varied systematically and extensively. A broad linear correlation of the bridging P–O(R) bond length and the pK_a of the substituent alcohol was observed. The results indicate that the P–O(R) bond changes by only ~0.04 Å with alcohol substituents that vary in pK_a by ~12 units, suggesting that phosphoryl group bonding responds in a subtle but regular manner to changes in the local environment. We also determined the effect on the phosphoryl bonding from changes in the solvent environment. Addition of dimethyl sulfoxide (DMSO) elongates the bridging bond, presumably as a result of lessened solvation to the nonbridging oxygens and conservation of bond order to phosphorus. Finally, we have addressed the relationship between ground-state bonding properties and reactivity, as changing the leaving group substituent and adding DMSO have large rate effects, and it was previously proposed that lengthening of the bond to be broken is the cause of the increased reactivity. The results herein suggest, however, that the change in the bridging bond energy is small compared to the changes in energy that accompany the observed reactivity differences. Further analysis indicates that electrostatic interactions can provide a common driving force underlying both bond lengthening and the observed rate increases. We suggest that ground-state distortions of substrates bound to enzymes can provide a readout of the electrostatic active site environment, an environment that is otherwise difficult to assess.

Introduction

Enzymatic catalysis is central to biological function, and much effort over the past decades has focused on elucidating the basic mechanisms of enzymatic catalysis. In recent years, approaches of molecular biology have readily allowed assessment of the catalytic effects of individual side chain mutations. Residues that give large effects upon mutation are typically found within active sites and most often appear to play direct roles in the

bond reorganization process.¹ For instance, these residues may act to form a covalent adduct, to abstract or donate a proton, or to hydrogen bond with a group that develops charge in the transition state. High-resolution X-ray structures of enzymes, especially in complex with substrates and transition-state analogues, have helped identify these residues and the interactions they make with the substrate. Thus, this structural information has served as a powerful aid in the development of coherent mechanistic descriptions of the reactions taking place within enzyme active sites.² However, enzymes are more than a collection of “catalytic residues”. A full understanding of their

* To whom correspondence should be addressed. E-mail: call@bioc.aecom.yu.edu and herschla@cmgm.stanford.edu.

[†] Department of Biochemistry, Albert Einstein.

[#] Department of Chemical Engineering, Stanford University.

[‡] Department of Biochemistry, Stanford University.

[§] Department of Molecular Pharmacology, Albert Einstein.

[⊕] Department of Chemistry, Stanford University.

[⊥] Present Address: Department of Diagnostic Radiology, Yale University.

^{||} Present Address: Marubeni America Corporation, New York.

[⊕] Present Address: Department of Biological Chemistry and Molecular Pharmacology, Harvard Medical School.

(1) (a) Plapp, B. V. *Methods Enzymol.* **1995**, 249, 91. (b) Gerlt, J. A. *Chem. Rev.* **1987**, 87, 1079.

(2) See, for example: (a) Muller, Y. A.; Schulz, G. E. *Science* **1993**, 259, 965. (b) Anderson, A. C.; Perry, K. M.; Freymann, D. M.; Stroud, R. M. *J. Mol. Biol.* **2000**, 297, 645. (c) Zechel, D. L.; Withers, S. G. *Acc. Chem. Res.* **2000**, 33, 11. (d) Schlichting, I.; Berendzen, J.; Chu, K.; Stock, A. M.; Maves, S. A.; Benson, D. E.; Sweet, B. M.; Ringe, D.; Petsko, G. A.; Sligar, S. G. *Science* **2000**, 287, 1615.

catalytic power must extend beyond the energetic view provided by rate effects from site-directed mutagenesis and the pictorial account of the bound reactants obtained by X-ray crystallography.

Polanyi, Pauling, Jencks, and others recognized that enzymes provide an environment that is preorganized for recognition of transition states and distinct from that in aqueous solution.³ However, the specific properties of active site environments have been more difficult to describe and understand. For example, there has been much discussion of the dielectric constant within enzyme active sites, as electrostatic interactions are generally more effective in a low dielectric environment.⁴ However, the dielectric constant describes a bulk property of a substance, whereas our interest is in describing the effects of the enzyme environment on substrates that are bound within the active site. Specific local and molecular interactions between the enzyme and the substrate determine the energetic effect of a change in charge distribution and therefore must be considered.⁵

The most common probe of local effects within enzymes and their active sites has been measurements of pK_a values.^{4c,6} These values can be measured in favorable cases and compared to those observed in water, the gas phase, and various organic solvents. Nevertheless, the observed pK_a is not simply a function of the electrostatic environment prior to protonation (or deprotonation). Upon protonation, for example, a hydrogen bond acceptor is converted to a hydrogen bond donor, and additional space is required to accommodate the transferred proton; the enzyme (or complex) therefore rearranges. Thus, the change in pK_a is a function of both the electrostatic environment preceding protonation and the ability of the site to rearrange to accommodate the newly protonated functional group.

Computation offers a nonperturbing approach to assess the electrostatic environment within an active site.⁵ While powerful in principle, limitations remain in the accuracy of computation and, as importantly, in the ability to test computation and connect it to relevant experimental observables.

In this work, we use nonenzymatic systems to show that vibrational spectroscopy can provide a sensitive probe of the environment of the phosphoryl group, a group commonly transferred in enzymatic catalysis. The bond order and length of the bridging P–O bond, the bond that is broken during the transfer reaction, appears to be accurately determined by vibrational spectroscopy. We have used Raman and infrared (IR) spectroscopy to determine the vibrational properties of the phosphoryl group for a series of monosubstituted phosphate dianions. We have also determined these properties for two phosphate esters as a function of solvent composition. The results provide a foundation for understanding both the bonding

behavior of monosubstituted phosphates and the electrostatic environment of the phosphoryl group, including that within enzyme active sites.

Materials and Methods

Chemicals. Disodium salts of *para*-nitrophenyl phosphate (pNPP)⁷ and phenyl phosphate (PP) were purchased from Aldrich and used without further purification. The disodium salt of methyl phosphate was obtained via hydrolysis of the methyl phosphorodichloridate with sodium hydroxide in excess. Dicyclohexylammonium salts of isopropyl phosphate, butyl phosphate, allyl phosphate, 2-methoxyethyl phosphate, 2-cyanoethyl phosphate, propargyl phosphate, 2,2,2-trifluoroethyl phosphate, 2,2,2-trichloroethyl phosphate, and 2,2,3,3,3-pentafluoropropyl phosphate were synthesized as previously described.⁸ Disodium salts of the above series of alkyl phosphates were obtained via anion exchange chromatography. Cyclohexylammonium salts of 4-cyanophenyl, 3-nitrophenyl, 4-bromophenyl, 4-fluorophenyl, and 4-methylphenyl phosphates were synthesized and characterized as previously described.⁹ 2-Aminoethyl, acetyl, 1-naphthyl, 2-naphthyl, glucose-1-, uridine-5-, guanosine-5-, glycerol-2-, glucose-6-, and inorganic phosphate, phosphorylcholine, and phosphoenolpyruvate were purchased from Sigma. Dimethyl sulfoxide (DMSO) and tetramethylammonium hydroxide (TMAH) were also purchased from Sigma. Sodium hydroxide (NaOH) and sodium chloride were purchased from Fisher.

Raman Spectroscopy. The Raman spectrometer used in these studies has been described in detail.¹⁰ Light at 568.2 nm at about 100 mW from a Coherent INNOVA 400-K3-krypton ion laser was used to excite Raman scattering from the sample. Scattered light was analyzed by a Triplemate spectrometer (Spex Industries, Metuchen, NJ) and detected by an optical multichannel analyzer (Model LN/CCD-1152UV detector with a ST-133 controller; Princeton Instrument, Princeton, NJ). Data were acquired, stored, and analyzed on a Macintosh IIfx computer (Apple, Cupertino, CA). All spectra were calibrated against the known Raman frequencies of toluene. Sample concentrations were 50 mM and spectra were taken at room temperature, unless noted otherwise.

FTIR Spectroscopy. IR absorbance spectra were measured with a Magna 760 Fourier transform spectrometer (Nicolet Instruments Corp., WI), using a MCT detector. A dual cell shuttle accessory was used to keep the sample and reference in identical environments to obtain difference spectra of the highest possible quality (discussed in detail in ref 11); this permits a sequential and repeated measurement of the sample and reference spectra. Spectra were collected in the range of 740–4000 cm^{-1} with BaF₂ cells and 25- μm spacers, although data below 900 cm^{-1} is obscured by the water and cell background. The resolution was set at 2 cm^{-1} and a Happ-Genzel apodization was applied. Temperature of the sample cell was controlled by a model RTE-111 (Neslab Instruments Inc.) bath circulator. Sample concentrations were 5 mM and spectra were taken at 25 °C, unless noted otherwise. For both Raman and FTIR measurements in aqueous solution, the pH was at least 1.5 pH units above the pK_{a2} for the compound, to ensure that the spectra of the dianion was monitored. No buffer was used in the sample. To ensure that the spectra of the dianion was monitored for mixed water/DMSO solutions, all the measurements were performed in 7–20 mM sodium or tetramethyl-

- (3) (a) Pauling, L. *Chem. Eng. News* **1946**, *24*, 1375. (b) Warshel, A. *J. Biol. Chem.* **1998**, *273*, 27035. (c) Jencks, W. P. *Catalysis in Chemistry and Enzymology*; McGraw-Hill: New York, 1969. (d) Fersht, A. *Enzyme structure and mechanism*; W. H. Freeman & Co.: New York, 1977. (e) Bruice, T. C.; Benkovic, S. J. *Biochemistry* **2000**, *39*, 6267. (f) Polanyi, M. Z. *Elektrochem.* **1921**, *27*, 142.
- (4) See, for example: (a) Rees, D. C. *J. Mol. Biol.* **1980**, *141*, 323. (b) Li, Y. K.; Kuliopulos, A.; Mildvan, A. S.; Talalay, P. *Biochemistry* **1993**, *32*, 1816. (c) Sternberg, M. J. E.; Hayes, F. R. F.; Russell, A. J.; Thomas, P. G.; Fersht, A. R. *Nature* **1987**, *330*, 86.
- (5) (a) Gilson, M. K.; Honig, B. H. *Nature* **1987**, *330*, 84. (b) Warshel, A.; Russell, S. T. *Q. Rev. Biophys.* **1984**, *17*, 283. (c) Lee, L. P.; Tidor, B. *Nat. Struct. Biol.* **2001**, *8*, 73. (d) Schaefer, M.; Karplus, M. *J. Phys. Chem.* **1996**, *100*, 1578.
- (6) See, for example: (a) Thornburg, L. D.; Henot, F.; Bash, D. P.; Hawkinson, D. C.; Bartel, S. D.; Pollack, R. M. *Biochemistry* **1998**, *37*, 10499. (b) Czerwinski, R. M.; Harris, T. K.; Massiah, M. A.; Mildvan, A. S.; Whitman, C. P. *Biochemistry* **2001**, *40*, 1984.

- (7) Abbreviations: DMSO, dimethyl sulfoxide; FTIR, Fourier Transform Infrared; MCT, Mercury-Cadmium-Telluride; NaOH, sodium hydroxide; pNPP, *para*-nitrophenyl phosphate; P–O, phosphorus–oxygen bond; P=O, the phosphorus–oxygen nonbridging bond (there are three such bonds in monosubstituted phosphates); P–O(R), the phosphorus–oxygen bond bridging the phosphate moiety with the leaving group for monosubstituted phosphates; PP, phenyl phosphate; TMAH, tetramethylammonium hydroxide; TS, transition state; ν , valence unit; ν , fundamental frequency; ν_a , antisymmetric stretch frequency; ν_s , symmetric stretch frequency.
- (8) Kirby, A. J. *Chem. Ind.* **1963**, 1877.
- (9) (a) Hall, A. D.; Williams, A. *Biochemistry* **1986**, *25*, 4784. (b) Zhang, Z.-Y.; Etten, R. L. V. *J. Biol. Chem.* **1991**, *266*, 1516.
- (10) Callender, R.; Deng, H. *Annu. Rev. Biophys. Biomol. Struct.* **1994**, *23*, 215.
- (11) Cheng, H.; Sukal, S.; Deng, H.; Leyh, T. S.; Callender, R. *Biochemistry* **2001**, *40*, 4035.

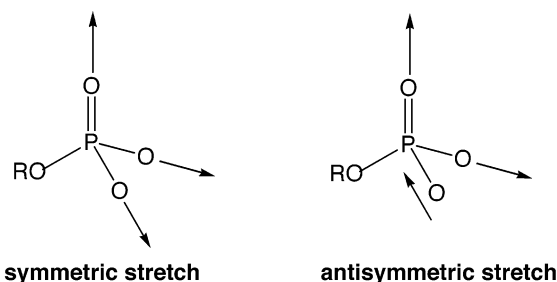


Figure 1. The symmetric and antisymmetric stretches of the P=O nonbridging bonds.

ammonium hydroxide (see Hydrolysis of *p*NPP and PP in DMSO). The IR measurements of each sample were completed within 20 min of sample preparation, to ensure that significant hydrolysis does not occur. The Raman measurements were performed in ~80 min.

Data Processing. Omnic 4.0a (Nicolet Instruments, Corp.) and Igor pro 3.1 (Wavemetrics Inc.) software were used to analyze and process the data. Spectra subtraction, second derivative, and Fourier self-deconvolution (FSD) were performed with the Omnic 4.0a software. As the conditions for the sample and reference measurements were the same, a direct subtraction of reference from sample usually resulted in a good difference spectrum. In particular, because water has no peak around the phosphate bands, a direct subtraction for spectra obtained in aqueous solution is reliable.¹¹ The spectrum of DMSO contains substantial absorbance at 1316 cm^{-1} and 1400–1450 cm^{-1} . Thus, small differences between the sample and reference can give spurious bands at these wavelengths. To remove spectral contributions from the DMSO peaks at 1316 cm^{-1} and 1400–1450 cm^{-1} for experiments in water/DMSO mixtures, the reference spectrum was multiplied by a factor slightly varying from one.

The antisymmetric stretching band of inorganic phosphate in the IR spectra is distinct from other bands, so that the frequency can be read directly from the spectrum. For monosubstituted phosphates on the other hand, the observed antisymmetric stretching band (Figure 1) exhibits small features on top of the otherwise smooth absorption band. In these cases, the C_{3v} symmetry of the $-\text{PO}_3^{2-}$ moiety has been lifted and the observed band is the superposition of two broad “antisymmetric-like” bands at slightly different frequencies. Two approaches were taken to obtain the frequency of the antisymmetric stretch, ν_a , in these cases. One was to take ν_a as the frequency at the center of the absorption band. The other was to determine the two-component antisymmetric-like stretch frequencies by calculation from the second derivative or by Fourier spectral deconvolution. The two approaches yielded the same value for bond lengths, using the formulas below, to within $\pm 0.001 \text{ \AA}$. Hence, the simpler method was adopted and the average antisymmetric stretch frequency is reported below. The only exception is *p*NPP, for which the positions of the antisymmetric bands were difficult to determine because the two antisymmetric modes overlap with a mode arising from the phenyl moiety. It was found useful in this case to employ Gaussian curve fitting of the FTIR spectra, using the peak positions found by second derivative and spectra deconvolution as initial peak placement. The corresponding Raman spectrum of *p*NPP was taken also to help identify the observed phenyl band in the phosphoryl antisymmetric stretch mode region, as this band was simultaneously Raman and IR active (unlike the antisymmetric stretch mode).

Hydrolysis of *p*NPP and PP in DMSO. Reactions were carried out with 50–200 μM *p*NPP (25 °C) or 200–500 μM PP (95 °C) and 1–20 mM sodium hydroxide or tetramethylammonium hydroxide in a series of water/DMSO mixtures. For *p*NPP, aliquots were removed and production of *p*-nitrophenolate was followed at 410 nm ($\epsilon = 1.82 \times 10^4 \text{ M}^{-1} \text{ cm}^{-1}$ at pH 10). For PP, inorganic phosphate formation was monitored using a modified molybdate assay.¹² It was necessary to carry

out reactions in glass vials, as reaction mixtures in Eppendorf tubes gave side products at elevated temperatures used to follow PP hydrolysis. For both *p*NPP and PP, reactions were first order in substrate, and rate constants were obtained by a nonlinear fit to a single exponential (Kaleidagraph, Synergy Software). End points of inorganic phosphate for PP reactions were routinely 50–80% of the total amount of starting phosphate ester (determined following total enzymatic hydrolysis with *E. coli* alkaline phosphatase), suggesting the occurrence of side reactions. This introduces uncertainty in the measured rate constants of on the order of ~2-fold. For both *p*NPP and PP, varying the hydroxide ion concentration over a 20-fold range gave effects of <2-fold on the observed rate constants, suggesting that hydrolysis of the dianion was being followed. The rate constants with tetramethylammonium hydroxide and sodium hydroxide were the same, within experimental error, suggesting that there were no ion specific effects. Control reactions with PP in which sodium chloride was used to maintain constant ionic strength gave the same rate constants, within error.

Results

The vibrational frequencies of the $-\text{PO}_3^{2-}$ moiety were used to determine the bond length and bond order of the bridging bond for a wide series of monosubstituted phosphates, $\text{RO}-\text{PO}_3^{2-}$, in aqueous solution and for two of these compounds in mixed water/DMSO solutions. In general, a highly accurate determination of bond lengths of small molecules in solution from vibrational frequencies is feasible (see below). This approach, however, has not seen wide use in recent years. For this reason, we provide an overview of how vibrational frequencies are related to bond lengths and bond orders.

Vibrational Data Analysis: General Principles. Gordy,¹³ on the basis of earlier work of Badger,¹⁴ established empirical correlations relating the frequencies of vibrational modes to bond length and bond order, through the force constant of the mode. These correlations hold up well for simple molecules or molecular fragments whose vibrational coordinates can be approximated as a diatomic oscillator; i.e., the measured frequency is proportional to the square root of the bond’s force constant divided by a suitable reduced mass. The accuracy of calculating a bond length from vibrational frequencies in these cases was as good as the accuracy of bond length measurements via crystallography, about 1% at the time of Gordy’s work.

In general, bond length versus frequency correlations are less accurate for polyatomic molecules. This is because interactions between nonbonded atoms show up as mode–mode coupling between internal coordinates of the molecule. Hence, the normal mode for a polyatomic molecule is typically not a simple diatomic oscillator but rather involves contributions from several internal coordinates. For phosphates of varying ionization states, including dianionic phosphate monoesters, the subject of this report, the normal modes of the stretch motions of nonbridging P=O bonds are not simple diatomic oscillators. For example, the individual frequencies of the dianionic phosphate symmetric, ν_s , and antisymmetric, ν_a , stretch modes (Figure 1) depend on the force constant and reduced mass of the relevant P=O bond and also on the molecule’s geometry and, to a lesser extent, other factors, such as off-diagonal coupling terms.¹⁵

Normal-mode analysis guided by ab initio calculations suggested an approach to isolate the properties of the P=O

(13) Gordy, W. *J. Chem. Phys.* **1946**, *14*, 305.

(14) Badger, R. M.; Bauer, S. H. *J. Chem. Phys.* **1937**, *5*, 839.

(15) Deng, H.; Wang, J.; Callender, R.; Ray, W. J. *J. Phys. Chem. B* **1998**, *102*, 3617.

(12) Taussky, H. H.; Shorr, E.; Kurzman, G. *J. Biol. Chem.* **1953**, *202*, 675.

bonds: in the geometric average frequency of the phosphate symmetric and antisymmetric stretch frequencies, geometrical contributions cancel one another. Thus, the geometrical mean is referred to as the “fundamental frequency”.¹⁵ The fundamental frequency, denoted as ν here, is then approximated as proportional to the square root of the P=O force constant divided by the reduced mass. Previous results with inorganic phosphate ions suggest that bond lengths can be determined to a high degree of accuracy via this approach.¹⁵ Below we describe how the fundamental frequency is obtained for monosubstituted phosphate dianions.

There are three independent nonbonded P=O stretch modes of the $-\text{PO}_3^{2-}$ moiety. For dianionic phosphate monoesters that preserve the C_{3V} symmetry of the $-\text{PO}_3^{2-}$ moiety, the normal modes are characterized by two doubly degenerate antisymmetric stretches, ν_a , located near 1110 cm^{-1} , and one symmetric stretch, ν_s , located near 970 cm^{-1} (Figure 1). The symmetric mode is allowed in Raman spectroscopy and weakly observed in the IR while the antisymmetric mode is allowed in IR and only weakly observed in Raman, allowing the above assignments. It is sometimes necessary to perform both Raman and IR spectroscopies to measure the symmetric and antisymmetric modes.

The fundamental frequency is given by

$$\nu = [(\nu_s^2 + 2\nu_a^2)/(3)]^{1/2} \quad (1)$$

For monosubstituted phosphates, the bond lengths of the three nonbridging P=O bonds are equal. When the C_{3v} symmetry is not retained, the degeneracy of the antisymmetric stretch modes is lifted, and three different frequencies are measured for the stretch modes of the $-\text{PO}_3^{2-}$ fragment. The fundamental frequency is then defined by

$$\nu = [(\nu_s^2 + \nu_{a1}^2 + \nu_{a2}^2)/(3)]^{1/2} \quad (2)$$

Typically, one of the bands is “symmetric-like” and the other two are “antisymmetric-like” in their polarization attributes as well as their relative band intensities in the Raman and IR spectra.

Vibrational Spectra, Fundamental Frequency, and Bond Orders and Lengths: Allyl Phosphate as an Example. Figure 2a shows the IR spectrum of allyl phosphate dianion. The relatively weak band near 980 cm^{-1} is assigned to the symmetric mode stretch of the nonbridging P=O bonds of the $-\text{PO}_3^{2-}$ fragment while the relatively stronger band near 1100 cm^{-1} represents the antisymmetric stretches. The 980 cm^{-1} band was observed in separate Raman measurements (data not shown), but the two antisymmetric modes were too weak to be observed in the Raman spectrum. The two antisymmetric-like modes in this spectrum are not at the same frequency, as two overlapping bands are evident near 1100 cm^{-1} . Second derivative analysis of the IR spectrum (Figure 2b) yields peak frequencies for the two antisymmetric modes of 1084 and 1109 cm^{-1} . The antisymmetric modes are not only more intense than the symmetric stretch, as expected in the IR spectrum, but also substantially broader. We have attributed this difference in bandwidth to the dependence of the symmetric and antisymmetric stretch frequencies on the O=P=O angle.^{15,16} The

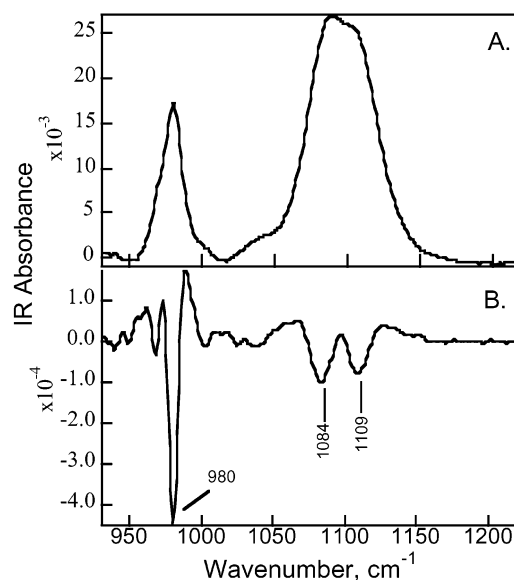


Figure 2. Vibrational spectra of allyl phosphate in an aqueous solution. (a) IR spectrum of allyl dianionic phosphate and (b) the corresponding second derivative spectrum. The spectrum is of 10 mM allyl phosphate in 20 mM NaOH at a resolution of 2 cm^{-1} .

O=P=O angle adopts a range of angles by thermal motion, and this results in a range of bond force constant values. These changes are additive for the antisymmetric mode frequency but cancel out for the symmetric mode.

The three frequencies for allyl phosphate, 980 , 1084 , and 1109 cm^{-1} , yield a fundamental frequency of $\nu = 1059\text{ cm}^{-1}$ using Equation 2. Using the average frequency of the antisymmetric stretches $\nu_a = 1096\text{ cm}^{-1}$, rather than the two peak frequencies revealed by the second derivative analysis, and $\nu_s = 980\text{ cm}^{-1}$ in Equation 1 yields the same value for ν .

Prior work comparing vibrational spectra and bond lengths derived from X-ray structures for crystals of inorganic phosphate and phosphate esters yielded the following empirical relationship between the fundamental frequency and length of the nonbridging bond (or average bond length in a nonsymmetrical $-\text{PO}_3^{2-}$ fragment):¹⁵

$$R_{\text{P=O}} = 0.2835 \text{ \AA} \cdot \ln(224500 \text{ cm}^{-1}/\nu) \quad (3)$$

The bond length of the nonbridging P=O bonds of allyl phosphate dianion is then calculated to be $R_{\text{P=O}} = 1.518\text{ \AA}$, using the fundamental frequency $\nu = 1059\text{ cm}^{-1}$ derived above.

Determination of Bond Order and Bond Length for the P–O(R) Bridging Bond: The Allyl Phosphate Example Continued. The intensity of the stretching mode of the P–O(R) bridging bond is typically substantially weaker than the nonbridging P=O vibrations. It is therefore difficult to measure, especially for compounds bound to proteins. In addition, while the bond lengths determined using an equation analogous to Equation 3 and the nonbridging P–O stretch frequencies have been empirically quite close to bond lengths determined from X-ray crystallography,¹⁵ the exact equation parameters have not been determined for calculating the bridging bond length using Equation 3. Nevertheless, this bond is often of primary interest, as it is the bond that is broken in many nonenzymatic and enzymatic reactions. We therefore outline an indirect approach, developed previously¹⁵ and used by us in several studies (e.g.,

(16) Wang, J.; Xiao, D.; Deng, H.; Webb, M. R.; Callender, R. *Biochemistry* **1998**, *37*, 11106.

ref 11 and 16), to estimate the bond order and bond length for the bridging P–O bond from the vibrational frequencies of the nonbridging bonds. Results described in a later section (Direct Measurement of the P–O(R) Bond Length of *p*NPP Using the P–O(R) Stretch) offer support for the accuracy of this approach.

The first step in determining the bridging bond order and length from the nonbridging P=O stretch frequencies rests on the network theory developed by Brown and co-workers as a refinement method for small molecule crystallography.^{17a–c} In this approach, the sum of the bond orders of all the bonds of a specific atom is fixed to the atomic valence; for phosphates this is 5.0. Although conservation of valence lacks theoretical basis, this bond valence paradigm has been shown to yield accurate bond length refinements in small molecule crystallographic studies and appears to have reasonable predictive value for modest changes.^{17a–c} In addition, analysis of crystal structures of a wide series of –PO₄ derivatives indicates that the sum of all the P–O bond lengths to a single phosphorus atom is nearly constant (6.177 ± 0.030 Å), providing specific support for the validity of conservation of valence for phosphorus.^{17d}

The second step of the analysis rests on relating bond order, bond length, and vibrational frequencies. The equation that defines the relationship between bond order and bond length for phosphates is¹⁵

$$S_{\text{P-O}}(\text{vu}) = (R_{\text{P-O}}/1.620 \text{ \AA})^{-4.29} \quad (4)$$

Furthermore, appropriate substitution of bond length derived in Equation 3 into Equation 4 yields the following relationship between the bond order of the P–O nonbridging bonds and the fundamental frequency:

$$S_{\text{P=O}}(\text{vu}) = [0.175 \cdot \ln(224500 \text{ cm}^{-1}/\nu)]^{-4.29} \quad (5)$$

$S_{\text{P-O}}$ is the bond order of the P–O bond (either bridging or nonbridging), $R_{\text{P-O}}$ is the length of the P–O bond (either bridging or nonbridging), and ν is the fundamental frequency for the nonbridging P=O bonds as defined above (Equations 2 and 3; in units of cm^{-1}). Equation 4 holds for either bridging or nonbridging bonds while Equation 5 holds only for the nonbridging bonds. When used to calculate bond order of the P–O(R) bridging bond, Equation 5 underestimates the bond order by about 5%, according to network theory.¹⁸ The total bond order of the nonbridging bonds in the –PO₃²⁻ fragment is therefore determined from empirical relationship in Equation 5, and the bond order of the bridging bond is then inferred by subtracting this number from 5. The bond length of the bridging P–O(R) bond is subsequently calculated through the use of Equation 4.

The value of $\nu = 1059 \text{ cm}^{-1}$ for allyl phosphate dianion (see previous section) yields an average bond order of $S_{\text{P=O}} = 1.320$ valence units (vu) for each of the three nonbridging P=O bonds using Equation 5. Multiplying 1.320 by three, for

Table 1. Vibrational Frequencies of the –PO₃²⁻ Moiety and the Derived P–O(R) Bond Length for a Series of Alkyl Phosphate Monoesters

alcohol substituent	pK _a ^a	ν_s^b (cm ⁻¹)	ν_a^c (cm ⁻¹)	ν^d (cm ⁻¹)	R_{bridging}^e (Å)
pentafluoro-2-propanol	10.1 ^f	983	1110	1069	1.616
phosphoenolpyruvate	11.1 ^g	976	1112	1069	1.615
trichloroethanol	12.2	981	1106	1066	1.612
trifluoroethanol	12.4	985	1112	1071	1.619
2-aminoethanol	12.65 ^h	981	1105	1065	1.612
2-propynol	13.6	980	1104	1064	1.611
choline	13.9	986	1103	1065	1.612
2-cyanoethanol	14.0 ⁱ	982	1100	1062	1.608
2-glycerol	14.4	978	1098	1060	1.605
2-methoxyethanol	14.8	981	1194	1058	1.603
2-propenol	15.5	980	1196	1059	1.605
methanol	15.5	983	1195	1059	1.605
butanol	16.1 ^j	973	1092	1053	1.599
2-propanol	17.1 ^j	971	1089	1050	1.596

^a The pK_a of the alcohol substituent is from ref 37, unless otherwise noted. ^b Symmetric mode frequency. ^c Doubly degenerate antisymmetric mode frequency. The average frequency is reported for cases in which the degeneracy of the two antisymmetric modes has been lifted. ^d Fundamental frequency (Equation 1). ^e Bond length of the bridging P–O(R) bond, calculated as described in the Results. ^f The pK_a of pentafluoroisopropyl alcohol is approximated on the basis of the pK_a values for the tri- and hexafluoro-2-propanol (from ref 37). Each additional fluorine atom is expected to lower the pK_a of the 2-propanol by ~0.8 pK_a units. ^g The pK_a of “the enol of pyruvate” is assumed to be equal to that of hydroxyethylene.⁴² ^h From ref 38. ⁱ From ref 39. ^j From ref 40.

the three P=O bonds, and subtracting the total from five yields 1.040 vu for the bridging P–O(R) bond. Use of $S_{\text{P-O}} = 1.040$ vu in Equation 4 gives a bridging bond length of 1.605 Å.

The accuracy in the absolute value of the bond lengths obtained from this method has been estimated to be ±0.004 Å on the basis of comparisons of spectroscopically determined bond lengths for methyl phosphate and triphenylphosphine oxide crystals to bond lengths from small molecule diffraction studies of these compounds.¹⁵ A large part of this error arises from mode–mode couplings between P=O stretches and other modes, which affect the character of the stretch mode. These couplings vary among the different phosphate compounds to some extent. An accuracy of ±0.004 Å corresponds to an error of ±13 cm^{-1} , using Equation 3 to relate frequency to bond length. The precision of the measurement of vibrational frequencies is much higher than this, about ±2 cm^{-1} , and the issue of mode–mode coupling is not as important for comparisons of the same molecule in different environments since the coupling parameters remain essentially constant. Hence, calculating bond length changes when a specific molecule undergoes a change in environment is expected to be more accurately determined. It is unclear what the accuracy is in that case as there are no experimental benchmarks, but an accuracy of better than ±0.001 Å is possible using the ultimate accuracy provided by the precision in the measurement of frequency. Finally, the conclusions drawn herein rely on the interpretation of the vibrational frequencies and would be unaffected by limitations in our ability to convert frequencies to accurate bond lengths.

Vibrational Spectra and Bridging P–O Bond Length for a Series of Monosubstituted Phosphates. Tables 1 and 2 tabulate the vibrational frequencies of the nonbridging P=O stretches, the calculated bridging P–O bond length, and the pK_a of the ROH substituent for several RO–PO₃²⁻ compounds, in aqueous solution. The vibrational data analysis employed was the same as that described above by way of example for the allyl phosphate dianion.

(17) (a) Brown, I. D.; Shannon, R. D. *Acta Crystallogr.* **1973**, *A29*, 3617. (b) Brown, I. D.; Wu, K. K. *Acta Crystallogr.* **1976**, *B32*, 1957. (c) Brown, I. D. *Acta Crystallogr.* **1992**, *B48*, 553. (d) Calleri, M.; Speakman, J. C. *Acta Crystallogr.* **1964**, *17*, 1097.

(18) Inherent to this error analysis is the assumption that the total bond order to phosphorus is equal to five (see refs 15 and 17a–c). The bond order of the bridging P–O(R) bond is underestimated by about 5% via the use of Equation 5, compared to the bond order calculated for the P–O(R) bridging bond by subtracting from five the total bond order for the P=O nonbridging bonds (calculated via the use of Equation 5).¹⁵

Table 2. Vibrational Frequencies of the $-\text{PO}_3^{2-}$ Moiety and the Derived P–O(R) Bond Length for a Series of Aromatic (A) and Other (B) Monosubstituted Phosphates

compound	$\text{p}K_a^a$	ν_s^b (cm^{-1})	ν_{a1}^c (cm^{-1})	ν_{a2}^c (cm^{-1})	ν^d (cm^{-1})	R_{bridging}^e (Å)
(A) aromatic phosphates						
4-nitrophenyl- PO_3^{2-}	7.1	983	1120	1076	1.625	
4-cyanophenyl- PO_3^{2-}	7.95	983	1118	1075	1.622	
3-nitrophenyl- PO_3^{2-}	8.4	985	1118	1076	1.622	
4-Br-phenyl- PO_3^{2-}	9.3	982	1108	1068	1.614	
1-naphthyl- PO_3^{2-}	9.3 ^f	980	1110	1068	1.615	
2-naphthyl- PO_3^{2-}	9.6 ^f	986	1112	1072	1.619	
phenyl- PO_3^{2-}	9.95	982	1108	1068	1.614	
4-F-phenyl- PO_3^{2-}	9.95	983	1109	1069	1.616	
4-methylphenyl- PO_3^{2-}	10.2	983	1108	1068	1.615	
(B) sugar phosphates and other phosphates						
glucose-1- PO_3^{2-}	12.4 ^g	968	1106	1062	1.608	
5'-GMP	14 ^h	978	1098	1060	1.605	
5'-UMP	14 ^h	980	1100	1062	1.608	
glucose-6- PO_3^{2-}	14.7 ^g	980	1095	1058	1.604	
acetyl- PO_3^{2-}	4.8	983	1130	1083	1.632	
HPO_4^{2-}	16.4 ⁱ	984	1084	1052	1.597	

^a The $\text{p}K_a$ of the alcohol substituent is from ref 37, unless otherwise noted. ^b Symmetric mode frequency. ^c Doubly degenerate antisymmetric mode frequency. The average frequency is reported for the cases in which the degeneracy of the two antisymmetric modes has been lifted. ^d Fundamental frequency (Equation 1). ^e Bond length of the bridging P–O(R) bond, calculated as described in the Results. ^f From ref 41. ^g From ref 38. ^h In the absence of experimental data, we approximate the $\text{p}K_a$ of the 5'-hydroxyl of guanosine and uridine to be ~ 14 . This is because the $\text{p}K_a$ for 2-methoxyethanol is 14.8, and the presence of 3'- and 2'-hydroxyls in the sugar moiety is expected to lower the $\text{p}K_a$ for the 5'-hydroxyl, relative to the $\text{p}K_a$ for the 2-methoxyethanol. ⁱ From ref 43.

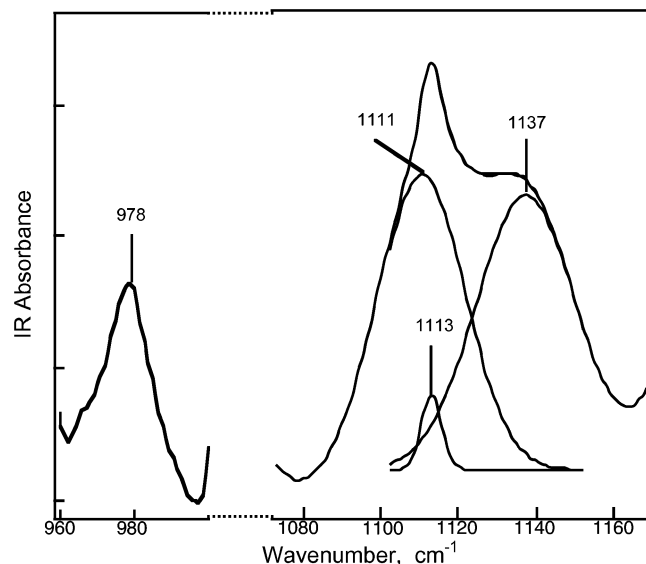


Figure 3. Vibrational spectra of *p*NPP in 50% DMSO/water solution. The spectrum between 1000 cm^{-1} and 1070 cm^{-1} is not shown because of the large absorbance of DMSO in this region. The spectrum is that of 5 mM *p*NPP and 7 mM TMAH, at room temperature, and the resolution is 2 cm^{-1} . The left band at 978 cm^{-1} corresponds to the symmetric P=O stretch of phosphate. The peak on the right, corresponding to the antisymmetric stretch, is composed of several bands. A Gaussian decomposition fit using three Gaussian functions is shown.

Bridging P–O Bond Length of *p*NPP and PP in Water/DMSO Mixtures. Figure 3 shows the IR spectra of *p*NPP in a 50% water/DMSO mixture. The symmetric stretch is located at 978 cm^{-1} . The spectrum in the antisymmetric mode frequency range is complicated. Gaussian curve fitting of the spectrum in this region revealed three overlapping peaks at 1111, 1113, and 1137 cm^{-1} (Figure 3). The small peak at 1113 cm^{-1} is assigned to a mode on the phenyl ring as a similar band shows up in the

Table 3. Vibrational Frequencies of the $-\text{PO}_3^{2-}$ Moiety and the Derived Bridging P–O(R) Bond Length of *p*NPP in Varying Amounts of DMSO Cosolvent

% DMSO	$\log(k_{\text{hyd}})^a$	ν_s^b (cm^{-1})	ν_{a1}^c (cm^{-1})	ν_{a2}^c (cm^{-1})	ν^d (cm^{-1})	R_{bridging}^e (Å)
0	−7.0	981	1111	1133	1077	1.625
25	−6.6	980	1110	1136	1077	1.625
50	−6.0	978	1110	1137	1077	1.625
60	−5.7	978	1112	1139	1078	1.627
70	−5.0	977	1113	1141	1079	1.628
80	−4.2	977	1119	1146	1082	1.632
90	−2.5	976	1125	1156	1088	1.638

^a The hydrolysis rate constant (k_{hyd}) in min^{-1} was measured as described in the Materials and Methods. ^b Symmetric mode frequency. ^c Two antisymmetric mode frequencies. ^d Fundamental frequency (Equation 2). ^e Bond length of the bridging P–O(R) bond, calculated as described in the Results.

Table 4. Vibrational Frequencies of the $-\text{PO}_3^{2-}$ Moiety and the Derived Bridging P–O(R) Bond Length of PP in Varying Amounts of DMSO Cosolvent

% DMSO	T (°C)	$\log(k_{\text{hyd}})^a$	ν_s^b (cm^{-1})	ν_a^c (cm^{-1})	ν^d (cm^{-1})	R_{bridging}^e (Å)
0	25	−9.4 ^f	981	1110	1968	1.615
0	95	−5.3 ^f	980	1111	1069	1.616
90	95	−2.8	975	1125	1077	1.625
95	95	−1.7	973	1131	1081	1.630

^a The hydrolysis rate constant (k_{hyd}) in min^{-1} was measured as described in the Materials and Methods, unless noted otherwise. ^b Symmetric mode frequency. ^c Doubly degenerate antisymmetric mode frequency (the average frequency is reported for the cases in which the degeneracy of the two antisymmetric modes has been lifted). ^d Fundamental frequency (Equation 1). ^e Bond length of the bridging P–O(R) bond, calculated as described in the Results. ^f The hydrolysis rate constant for the aqueous reaction has been extrapolated on the basis of a series of measurements at higher temperatures (O'Brien, P. J.; Wolfenden, R.; Herschlag, D. unpublished results).

spectrum of phenyl phosphate. The two strong bands at 1111 and 1137 cm^{-1} are assigned to the two antisymmetric-like vibrations of the nonbridging P=O bonds. Substituting 978, 1111, and 1137 cm^{-1} into Equation 2 for ν_s , ν_{a1} , and ν_{a2} yields a fundamental frequency of $\nu = 1077 \text{ cm}^{-1}$. The P–O(R) bond lengths can then be determined as described above (Determination of Bond Order and Bond Length for the P–O(R) Bridging Bond: The Allyl Phosphate Example Continued).

Table 3 lists the measured hydrolysis rate constants for *p*NPP in various water/DMSO mixtures at 25 °C. The rate constant is highly sensitive to the DMSO content, increasing dramatically for DMSO concentrations greater than 70–80%, as previously noted.¹⁹ Also given in Table 3 are the nonbridging phosphate stretch modes (see Figure 3 for the 50/50% spectrum), the calculated fundamental frequency, and the calculated bridging bond length (see above). Table 4 provides the hydrolysis rate constants for phenyl phosphate (see Materials and Methods). The measured frequencies are quite insensitive to temperature while the hydrolysis rate constants are quite sensitive. This is expected if temperature has little effect on the structure of the ground state but simply raises the percentage of molecules with sufficient energy to cross the transition-state barrier.

Direct Measurement of the P–O(R) Bond Length of *p*NPP Using the P–O(R) Stretch. The bond length of the bridging P–O(R) bond can be estimated directly from Equation 3, using the same parameters derived for the nonbridging bonds. The frequency of the bridging bond stretch is then substituted for the fundamental frequency, ν . We estimate that the bond length

(19) (a) Abell, K. W. Y.; Kirby, A. J. *Tetrahedron Lett.* **1986**, 27, 1085. (b) Grzyńska, P. K.; Czuryca, P. G.; Golightly, J.; Small, K.; Larsen, P.; Hoff, R. H.; Hengge, A. C. *J. Org. Chem.* **2002**, 67, 1214.

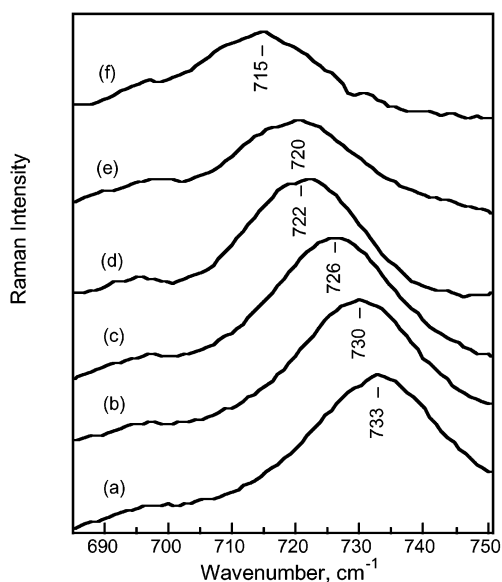


Figure 4. The Raman spectra of the P–O(R) stretch of pNPP in DMSO/water mixtures, (a) to (f): 0, 20, 50, 60, 70, and 80% DMSO. 6-Deuterated DMSO was used to avoid the high Raman signal from protonated DMSO in this region. The spectra are of 10 mM pNPP in 20 mM NaOH at a resolution of 6 cm^{-1} .

Table 5. Comparison of the P–O(R) Bridging Bond Lengths Determined from the Analysis of the Nonbridging Bond Vibrational Modes and from Direct Analysis of the P–O(R) Bond Vibrational Mode

% DMSO	ν_{bridging}^a (cm^{-1})	R_{bridging}^b (Å)	R_{bridging}^c (Å)	$R_{\text{bridging}} - R_{\text{bridging}}^c$ (Å)
0	733	1.623	1.625	–0.002
25	730	1.624	1.625	–0.001
50	726	1.626	1.625	0.001
60	722	1.627	1.627	0.000
70	720	1.628	1.628	0.000
80	715	1.630	1.632	–0.002

^a Stretching frequency of the bridging P–O(R) bond of pNPP in various water/DMSO solutions (data presented in Figure 4). ^b Bond length of the bridging P–O(R) bond, calculated directly from Equation 3 and the stretching frequency of the bridging P–O(R) bond. ^c Bond length of the bridging P–O(R) bond, calculated from the nonbridging bond stretch frequencies using Equations 4 and 5, as discussed in the Results. Values are from Table 3.

of the P–O(R) bond derived from the direct use of Equation 3 will yield results that underestimate the P–O(R) bond length by $\sim 0.2\%$, on the basis of comparisons with crystallographic data for model compounds.¹⁵ Figure 4 shows the Raman spectra of pNPP in various water/DMSO mixtures in the region of the P–O(R) bridging bond stretch (Raman spectroscopy is used since this mode is highly obscured by solvent and cell background in the IR). Table 5 gives the values of the bridging P–O(R) stretch frequency for pNPP in water/DMSO mixtures and the P–O(R) bond length, $R_{\text{P–O(R)}}$, calculated using the bridging P–O(R) stretch frequency directly as ν in Equation 3. Also tabulated is the bond length, $R_{\text{P–O(R)}}$, derived from Equations 4 and 5, using the frequencies associated with the nonbridging bonds and the network theory, as described above. The bond lengths derived from the two procedures are in close agreement.

These results validate two important points. First, the bond order of the bridging P–O(R) bond does indeed weaken as the amount of DMSO is increased. The P–O(R) stretch frequency is directly correlated to the electron density in the bond so that a lower frequency means a smaller bond order. In addition, the

comparison shows that consistent values of the bridging bond length are obtained from the two methods.

Discussion

Phosphoryl transfer is likely the most common class of reactions in biology. Decades of study of phosphoryl transfer by structure–reactivity approaches have provided much insight into these reactions and their transition states.^{20,21} To further our understanding of how phosphoryl compounds react, we have focused on determination of basic properties of these compounds, and to further our understanding of how phosphoryl transfer reactions are catalyzed, we have focused on understanding the environment at the site of catalysis.

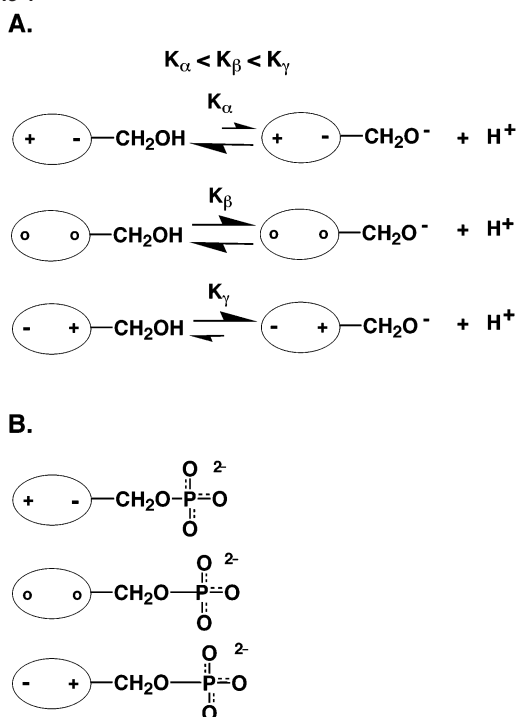
Vibrational spectroscopy offers a unique and direct probe of the actual bonding and bond properties of phosphoryl compounds. Previous work and the results described herein suggest that properties of the nonbridging bonds of the phosphoryl group can be ascertained to high precision ($\pm 0.004\text{ Å}$), despite the occurrence of complex vibrational modes; this is accomplished by appropriate combination of the observed phosphoryl vibrational modes. Assuming only a conservation of the valence bond order for the phosphorus atom, this analysis can be extended to yield the bonding properties of the P–O(R) bridging bond—the bond that is broken during phosphoryl transfer (see ref 15 and Results herein). The ability to obtain P–O(R) bridging bond lengths via this analysis, which are in agreement with those obtained by direct consideration of the stretching vibrational mode of the P–O(R) bridging bond within experimental error, provides further support for this approach.

In the sections that follow, we address what has been revealed about the fundamental properties of the P–O(R) bridging bond and the applicability of vibrational spectroscopy as a sensitive probe for the electrostatic environment of the phosphoryl group. First, we describe bonding properties derived from vibrational spectroscopy for a series of monosubstituted phosphoryl compounds, in which the phosphoryl substituent has been varied systematically and extensively. Next, we describe phosphoryl bonding changes due to variation of the solvent environment, also derived from vibrational spectroscopy. We then discuss the relationship between the ground-state bonding properties and reactivity. Finally, we discuss implications of this work for enzymatic catalysis.

Substituent Effects on Phosphoryl Group Bonding: Correlation of the Bridging P–O(R) Bond Length with Substituent $\text{p}K_{\text{a}}$. Kirby and co-workers carried out a systematic small molecule crystallography study, probing bonding for a series of substituted aryl acetals. The results suggested that substituents that lowered the $\text{p}K_{\text{a}}$ of the aryl group stabilized a longer C–O(R) bond,^{22,23} presumably because of electron-withdrawing effects that lessen the electron density on the oxygen atom and thereby weaken the bond or through-space substituent effects that electrostatically stabilize greater electron

- (20) (a) Cleland, W. W.; Hengge, A. C. *FASEB J.* **1995**, *9*, 1585. (b) Benkovic, S. J.; Schray, K. J. In *Transition States of Biochemical Processes*; Gandour, R. D., Schowen, R. L., Eds.; Plenum: New York, 1978; p 493. (c) Williams, A. J. *Am. Chem. Soc.* **1985**, *107*, 6335. (d) Thatcher, G. R. J.; Kluger, R. *Adv. Phys. Org. Chem.* **1989**, *25*, 99.
- (21) Hengge, A. C. In *Comprehensive Biological Catalysis*; Sinnott, M. L., Ed.; Academic Press: London, 1998; p 517.
- (22) (a) Allen, F. H.; Kirby, A. J. *J. Am. Chem. Soc.* **1984**, *106*, 6197. (b) Briggs, A. J.; Glenn, R.; Jones, P. G.; Kirby, A. J.; Ramaswamy, P. *J. Am. Chem. Soc.* **1984**, *106*, 6200.
- (23) Jones, P. G.; Kirby, A. J. *J. Am. Chem. Soc.* **1984**, *106*, 6207.

Scheme 1



density on the oxygen atom and thereby preferentially stabilize a longer C–O(R) bond. An analogous correlation was suggested for phosphoryl compounds,²³ but acquiring data for an extensive series of phosphoryl compounds is hampered by the difficulty in crystallizing these compounds in homologous crystal environments. For this reason and because vibrational studies can be carried out in and compared between solution, protein, and crystal environments, we have turned to Raman and IR spectroscopy of a series of phosphoryl compounds to probe the bonding properties of the phosphoryl group in aqueous solution.

In the simplified model of Scheme 1, the alkyl substituents of dianionic alkyl phosphate monoesters are schematically and approximately represented as dipoles.²⁴ The greater the positive charge potential from this dipole, the lower the pK_a of the alcohol, as the dipole provides greater stabilization of the negative charge present in the alkoxide but not the alcohol. Analogously, as the P–O(R) bond lengthens, negative charge accumulates on the bridging oxygen, all other factors being equal. (This can be thought of as a greater contribution from an alkoxide ion resonance form.) Thus, there is a simple prediction that the P–O(R) bond will lengthen as the pK_a of the alcohol substituent decreases. Nevertheless, the extent of bond lengthening from this effect could not be predicted, nor was it apparent if the effect would be large enough to detect or if other factors idiosyncratic to the individual alkyl phosphate dianions would obscure the predicted trend.

Figure 5 shows the bond length for the bridging P–O(R) bond, derived from vibrational spectra (Table 1 and Results), plotted as a function of the pK_a of the alcohol substituent for a

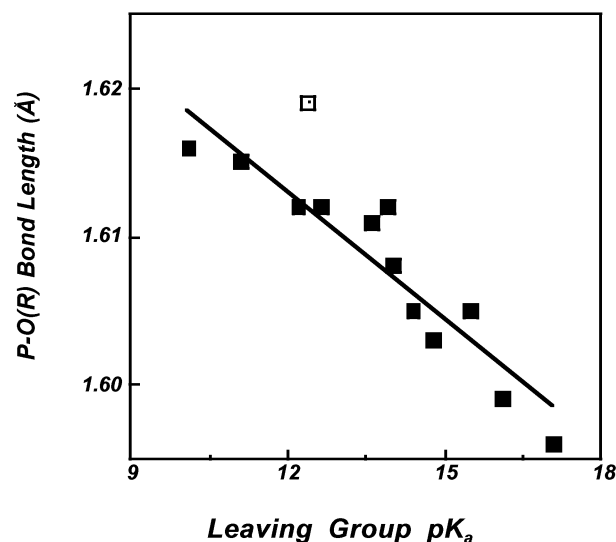


Figure 5. The bond length of the bridging P–O(R) bond for alkyl phosphate monoesters, $RO-PO_3^{2-}$, plotted as a function of the pK_a of the alcohol (ROH) substituent. The data are taken from Table 1 for a series of alkyl phosphates, the point for trifluoroethyl phosphate is depicted by the open symbol. The line is a least-squares fit to the data; excluding the trifluoroethyl phosphate data point⁴⁴ gives $R(\text{Å}) = 1.647 - 0.00284 \cdot pK_a$, with the correlation coefficient $R^2 = 0.87$. Inclusion of trifluoroethyl phosphate gave $R(\text{Å}) = 1.650 - 0.00304 \cdot pK_a$, with the correlation coefficient $R^2 = 0.82$.

series of simple alkyl phosphate dianions. There is a linear increase in the bond length as the substituent pK_a decreases, suggesting that phosphoryl group bonding responds in a regular manner.

Given this trend, we next determined whether an extended correlation could be obtained for a wider variety of monosubstituted phosphoryl compounds. Figure 6 presents data for the alkyl phosphates as well as several aryl phosphates, more complex alkyl phosphates, and inorganic phosphate, as a function of the pK_a of the phosphoryl substituent. A single line gives a good fit to all of the data, spanning a range of substituent pK_a values of >12 units (see Figure 6 legend). The slope of this line is $\sim 0.003 \text{ Å}/(pK_a \text{ unit})$. Nevertheless, there may be small differences in the dependencies for the alkyl and aryl phosphates and the deviations may arise because of different mechanisms underlying the pK_a effects (such as inductive versus resonance).

The slope of the correlation in Figure 6 is of the same order of magnitude as the slope of $\sim 0.006 \text{ Å}/(pK_a \text{ unit})$ estimated from the previous limited X-ray data,²³ although a direct comparison is difficult because of the following: the lower dielectric and different local environment in the crystal compared to aqueous solution, the effects of different counterions and crystal forms on the bond lengths for the four compounds used in the X-ray correlation, and the relatively large uncertainty in the bond lengths determined crystallographically (standard deviations of ± 0.005 to $\pm 0.02 \text{ Å}$).²³ The possibility of systematic errors in determination of bond lengths from vibrational data has also not been rigorously eliminated.

The phosphoryl substituents span of 12.3 pK_a units corresponds to a $\Delta\Delta G$ of 16.8 kcal/mol for the deprotonation equilibrium to form the oxyanion.²⁶ Thus, a group that stabilizes the oxyanion by ~ 17 kcal/mol lengthens the P–O–(R) bond by only $\sim 0.04 \text{ Å}$. As described in the following sections, the relationship of these parameters to changes in reactivity and to

(24) We use a simplified model to understand stabilization of the leaving group alkoxide ion substituent. Several studies have suggested that substituents in nonconjugated systems exert their effects predominantly through space rather than through the bonded chain (see, for example, ref 25 and references therein), so that consideration of substituents as attached dipoles, as in Scheme 1, may provide a reasonable representation. This approximation is useful conceptually for the treatment presented in the text, but it is not required for the conclusions that are drawn. For instance, for conjugated systems, resonance effects are likely important.

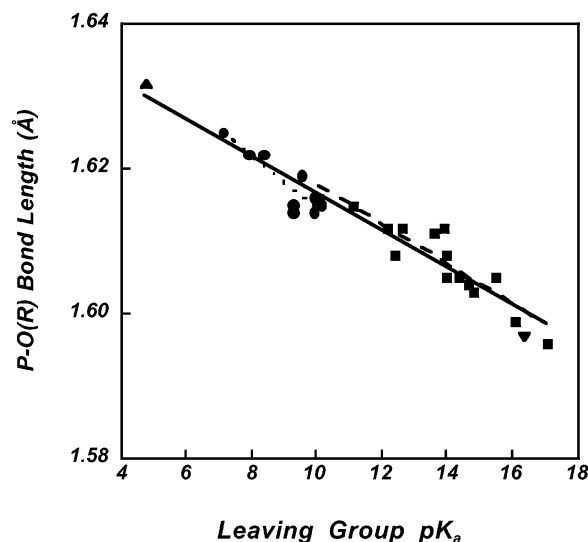


Figure 6. The bond length of the bridging P–O(R) bond for various monosubstituted phosphates, RO–PO₃²⁻, plotted as a function of the pK_a of the ROH substituent. The data are taken from Table 1 and Table 2B for alkyl phosphates (■), Table 2A for aromatic phosphates (●), and Table 2B for acetyl phosphate (▲) and inorganic phosphate (▼). The solid line is a least-squares fit to all the data: R (Å) = 1.642 – 0.00257 · pK_a, with the correlation coefficient R^2 = 0.92. The dotted line is a least-squares fit to the aromatic phosphates data: R (Å) = 1.650 – 0.00356 · pK_a, with the correlation coefficient R^2 = 0.80. The dashed line is a least-squares fit to the alkyl phosphate data from Tables 1 and 2B, excluding trifluoroethyl phosphate.⁴⁴ R (Å) = 1.645 – 0.00275 × pK_a, with the correlation coefficient R^2 = 0.83.

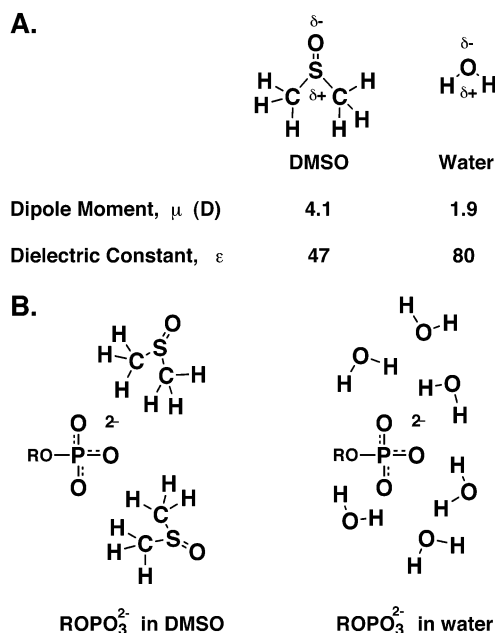
more general changes in environment may contribute to our fundamental understanding of these reactions, of the enzyme active environment, and the ability of this environment to provide transition-state stabilization via electrostatic interactions (see Implications for Reactivity of Phosphoryl Compounds and Implications for Enzymatic Catalysis below). In addition, vibrational spectra and their response to substituents and environmental changes provide incisive physical descriptions of monosubstituted phosphoryl compounds that may provide critical guides and decisive tests of future computational models.

Environmental Changes and Phosphoryl Group Bonding: The Effect of DMSO on the Bridging P–O(R) Bond Length. We have used the addition of DMSO as a cosolvent to directly probe the effect of changes in the environment surrounding the phosphoryl group on its bonding. This general question is of particular importance for understanding enzymatic catalysis, as enzymes create an idiosyncratic environment within which catalysis takes place (see Introduction and Implications for Enzymatic Catalysis below). DMSO was chosen because it is compatible with IR and Raman spectroscopy and because DMSO addition was previously shown to exert a large rate effect on the hydrolysis of a phosphate ester, pNPP.¹⁹

Upon addition of DMSO, the P–O(R) bridging bond lengths for both pNPP and PP (Tables 3–5). The changes are small (=0.015 Å), but there is a steady trend as the amount of DMSO cosolvent is increased.

Scheme 2 presents a crude model that can account for this trend. Despite the high dielectric constant of DMSO solutions

Scheme 2



(Scheme 2), DMSO is poor at solvating anions, such as the nonbridging phosphoryl oxygen atoms (see, for example ref 27). This limitation presumably arises because the positive end of the DMSO dipole is sequestered behind the two methyl groups (Scheme 2A). This limits both the close approach of the dipole and the number of DMSO molecules that can align around the phosphoryl group. The lessened favorable electrostatic interactions with the nonbridging phosphoryl oxygen atoms upon addition of DMSO will favor states with less charge accumulation on these atoms; this provides an energetic “incentive” to shorten these bonds (Scheme 2B). Analysis of the “fundamental frequency” described in the Results indicates that as the fraction of DMSO in the solvent increases, the nonbridging P–O bonds are indeed shortened by a small but readily measurable amount. Shortening of these bonds is equivalent to an increase in double-bond character, and, given conservation of bond order around phosphorus, the bond order of the bridging P–O(R) bond decreases and this bond lengthens (Tables 3 and 4). Vibrational spectra probing the stretching mode for the bridging bond provide direct and independent support for this conclusion (see Table 5 and Direct Measurement of the P–O(R) Bond Length of pNPP Using the P–O(R) Stretch in Results).

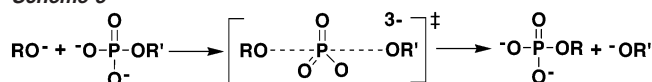
In summary, bonding of the phosphoryl group responds to the environment. This is observed directly in the DMSO effects. The effect of substituents on phosphoryl bonding, described in the previous section, can also be considered as a model for environmental effects. In this model, a series of dipoles were introduced intramolecularly and varied regularly; in enzymes, the active site environment includes several dipolar, charged, and hydrophobic groups; the sum of these interactions defines the environment of the reactive group (see Implications for Enzymatic Catalysis below).

Implications for Reactivity of Phosphoryl Compounds. The phosphoryl substituents described in Scheme 1 that lengthen

(25) (a) Cole, T. W.; Mayers, C. J.; Stock, L. M. *J. Am. Chem. Soc.* **1974**, *96*, 4555. (b) Petti, M. A.; Sheppard, T. J.; Barrans, R. E.; Dougherty, D. A. *J. Am. Chem. Soc.* **1988**, *110*, 6825. (c) Cozzi, F.; Cinquini, M.; Annunziata, R.; Siegel, J. S. *J. Am. Chem. Soc.* **1993**, *115*, 5330.
(26) (a) $K_1/K_2 = 10^{(17.1-4.8)} = 10^{12.3}$; $\Delta\Delta G = RT \ln(K_1/K_2) = 16.8$ kcal/mol (at 298 K).

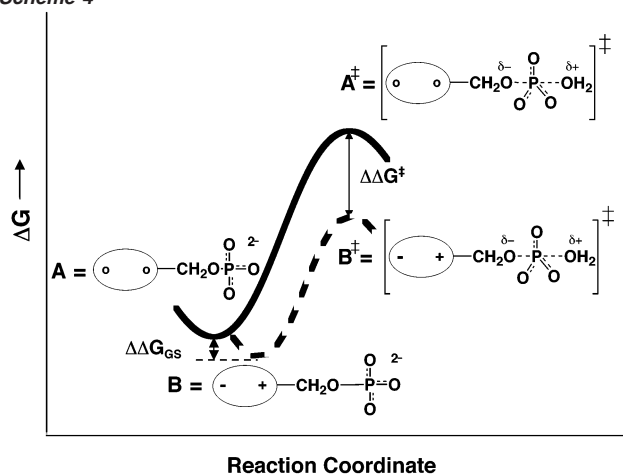
(27) (a) Kolthoff, I. M.; Chantooni, M. K., Jr.; Bhowmik, S. *J. Am. Chem. Soc.* **1967**, *90*, 23. (b) Matthews, W. S.; Bares, J. E.; Bartmess, J. E.; Bordwell, F. G.; Cornforth, F. J.; Drucker, G. E.; Margolin, Z.; McCallum, R. J.; McCollum, G. J.; Vanier, N. R. *J. Am. Chem. Soc.* **1975**, *97*, 7006. (c) Bordwell, F. G. *Acc. Chem. Res.* **1988**, *21*, 456.

Scheme 3



the P–O(R) bridging bond increase the rate of breaking of that bond in phosphoryl ($-\text{PO}_3^{2-}$) transfer reactions (Scheme 3). DMSO, which lengthens the P–O(R) bridging bond in *p*NPP and PP, also increases the rate of phosphoryl transfer (Tables 3 and 4 and ref 19). Thus, bond length correlates with reaction rate. Kirby, and more recently Hengge, suggested that the increase in bond lengths might be the cause of the increased reaction rates.^{23,19b} More generally, it is important to ascertain, for any correlation, whether there is a cause–effect relationship, a common underlying causative feature, or simply a coincidence. The following analyses suggest that the magnitude of the effects on reactivity is much larger than can be accounted for by weakening of the bridging bond. Instead, the data and correlations are readily accounted for by a common underlying mechanism based on stabilization of negative charge on the bridging oxygen leaving group alkoxide or phenoxide ion. Such effects can in certain cases be described solely by electrostatic interaction energies.

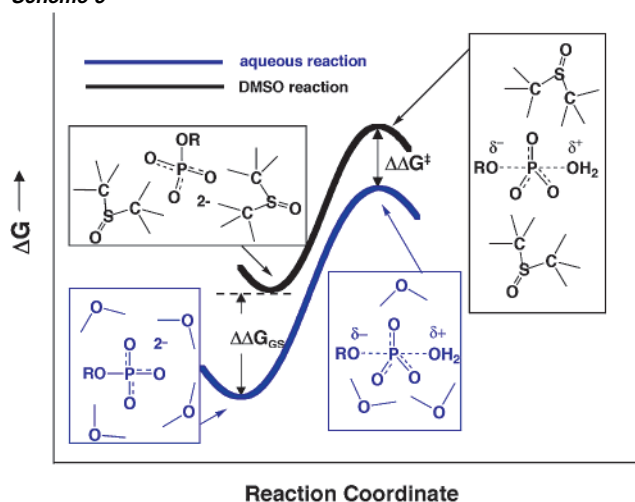
Scheme 4



Scheme 4 shows a free-energy-reaction coordinate diagram for two phosphate esters that vary in reactivity because of a substituent on the leaving group alcohol.²⁸ As in Scheme 1 above, the substituent interacts energetically with the bridging oxygen. We assume a (small) partial negative charge on this oxygen atom so that the substituent dipole that lowers the leaving group pK_a would have a small favorable interaction in the ground state; this would lower the free energy of compound B relative to compound A, all other factors being equal. This is represented by the slightly lower free-energy position for compound B in Scheme 4. As described above (Scheme 1 and Substituent Effects on Phosphoryl Group Bonding: Correlation of the Bridging P–O(R) Bond Length with Substituent pK_a), the substituent dipole is expected to lengthen the P–O(R) bond, as is observed; we therefore also depict compound B's ground state as further advanced along the reaction coordinate than compound A's ground state. It is this movement along the reaction coordinate that led to the suggestion that bond

(28) The free-energy reaction profile is grossly simplified, with only one coordinate depicting the reaction progress.

Scheme 5



lengthening is causative of the observed rate enhancement. Consideration of the energetics of the substituent oxygen interactions, however, leads to a different conclusion.

In the transition state for transfer of the $-\text{PO}_3^{2-}$ group, the bond to the leaving oxygen atom is nearly broken, as judged by linear free-energy relationships, kinetic isotope effects, and measurements of entropy and volume of activation (Scheme 3).^{20,21} Thus, a nearly full negative charge is expected to reside on this oxygen atom in the transition state. Because of the large increase in negative charge potential at the bridging oxygen position in the transition state, the interaction energy with the substituent dipole is expected to be much larger in the transition state than in the ground state. Thus, the reaction rate will increase for the same reason underlying the bond lengthening: the electrostatic interaction energy (Schemes 1 and 4).

Analogous considerations hold for the DMSO result (Scheme 5).²⁸ As noted above, DMSO is less effective than water at solvating localized negative charges. Thus, the free-energy change for transfer of a phosphoryl group from water to DMSO is unfavorable.²⁹ In the transition state, charge is presumably dispersed, relative to the ground state.^{21,30} This charge dispersal can occur despite the increase in charge density on the leaving group oxygen. A decrease in charge on the three nonbridging oxygen atoms and the ability of the aromatic ring to partially disperse charge accumulated on the bridging oxygen atom presumably both contribute to the charge dispersal in the transition state. Thus, the energy penalty for transfer of the transition state from water to DMSO is expected to be less than that for the ground state. That is, the weaker solvation of charge on the phosphoryl oxygens by DMSO relative to water is expected to both lengthen the P–O(R) bridging bond, as described above (Scheme 2), and lower the free-energy barrier for reaction. Apparently, the solvation differences between water and DMSO, traceable to electrostatic interaction differences, are responsible for both the longer P–O(R) bonds and the faster reactions in DMSO.

(29) The attached alkyl group of the phosphate ester is ignored in this treatment. This is because the phosphate ester can vary in differential solubility in water versus DMSO depending on the alkyl group used, but this alkyl chain is, to a reasonable approximation, unchanged in going from the ground state to the transition state. As we are focused on reactivity, we do not consider this portion of the phosphate ester.

(30) (a) Herschlag, D.; Jencks, W. P. *J. Am. Chem. Soc.* **1989**, *111*, 7579. (b) Westheimer, F. H. *Chem. Rev.* **1981**, *81*, 313.

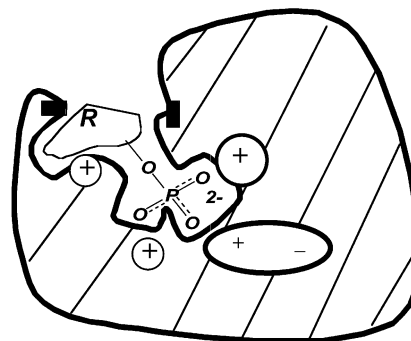
It is notable, from Schemes 4 and 5, that in one case (the substituent effect) both the ground state and the transition state can be stabilized from the interaction of the substituent oxygen with the dipole, but the transition state is stabilized more, whereas in the other case (the DMSO effect) both the ground state and the transition state can be destabilized because of the addition of DMSO, but the ground state is destabilized more.

Another way of addressing the relationship between reactivity and bond length is to consider the energetic perturbation of the bridging bond over the correlation range for both the substituent and the DMSO effect (Figure 6 and Table 3). The hydrolysis rate is expected to change by ~ 15 orders of magnitude over a 12 $\text{p}K_{\text{a}}$ unit range.³¹ This corresponds to a ~ 20 kcal/mol difference in the free energy of activation for the compounds at the extremes of the $\text{p}K_{\text{a}}$ range. Ninety percent DMSO increases the reaction rate of *p*NPP by $3 \cdot 10^4$ fold (Table 3), which corresponds to 6.2 kcal/mol of the free energy of activation difference. The ~ 0.04 Å difference in the ground-state bond length of the P–O–(R) bond observed over the leaving group $\text{p}K_{\text{a}}$ range or the ~ 0.01 Å bond length change observed for the water/DMSO study represents very small distortions of the bridging bond in energetic terms. For example, for a small distortion of the bridging P–O bond the change in potential energy of the molecule is given by $(1/2) \cdot k \cdot (R - R_0)^2$, where k is the force constant and R_0 is the bond length at minimum energy. The force constant is calculated from the frequency of the P–O stretch mode and the reduced mass of this internal coordinate. Using $k = 334$ N/m obtained from the frequency of 733 cm^{-1} observed for *p*NPP in aqueous solution (Table 5), a 0.04 and a 0.01 Å distortion (i.e., $(R - R_0)$) yield a potential energy change of 0.4 and 0.02 kcal/mol, respectively. This is in general agreement with ab initio quantum mechanical calculations which suggest that a 0.1 Å elongation of a bridging P–O(R) bond corresponds to forces that bring to bear a stress on the bond of only ~ 1 kcal/mol.¹¹ Thus, the energy change in the barrier to reaction is much greater than the bond energy difference in both correlations.

Finally, the relationship between bond length in the ground state and reactivity can also be addressed by considering the following thought experiment. There are cases of phosphoryl transfer reactions with the same leaving group that involve different amounts of bond cleavage in the transition state. This is the case for reactions involving pyridine leaving groups, which give Brønsted values $\beta_{\text{leaving group}} = -1.02$ and -0.79 for reactions with water and hydroxide ion, respectively.³² This means that a fixed set of phosphoryl compounds with a fixed set of ground-state bond lengths has different relative reaction rates, depending on the nature of the nucleophile used in the reaction. The ability to have different rate effects from a common change in bond length indicates that the change in bond length is not fully causative of the observed changes in reactivity.

In summary, we suggest that the correlations between bond lengths and reactivity are neither a coincidence nor indicative of a causative relationship between bond length and reactivity. Rather, the same electrostatic interaction energies provide a

Scheme 6



common driving force in both lengthening the P–O(R) bond and in increasing the reaction rates.

Implications for Enzymatic Catalysis. Vibrational spectra have been obtained for ligands of several enzymes, revealing bonding properties within active site environments.³³ The results herein concerning bonding of phosphoryl compounds and their solution reactivity have implications for enzymatic catalysis and its mechanistic dissection. They underscore the potential of vibrational spectroscopy for future investigation of enzymatic phosphoryl transfer, as the P–O bond is highly sensitive to its surroundings and can be well-characterized by vibrational spectroscopy. The results herein also provide a series of standards to gauge the behavior of phosphoryl compounds within active sites and potentially to unravel catalytic contributions. Finally, the underlying origin of relationships between ground-state bond distortions and reactivity described herein has implications for understanding ground-state destabilization in enzymatic catalysis. Each of these points is discussed briefly below.

By definition enzymes are designed to provide preferential stabilization of transition states relative to ground states; this is simply the definition of catalysis according to transition-state theory. For phosphoryl transfer, groups in and around the active site, which create a positive potential at the position of the leaving group oxygen atom, can stabilize the charge buildup on this atom in the transition state (Scheme 6). The dipolar substituents of the series of alkyl phosphates described above provide a simplified model for this effect, showing that the P–O(R) bond is affected by its environment (Scheme 1 and Figure 5). Thus, the extent of perturbation of this bond may provide a readout of the electrostatic environment within the active site. As emphasized in the Introduction, this critical catalytic feature is difficult to probe by traditional means.

Quantitating contributions from individual catalytic mechanisms has been notoriously difficult in enzymology, in large part because of the interdependence of active site interactions; for example, mutating a residue that acts as a general base can also affect the alignment of substrates in the active site. The ability of vibrational spectroscopy to probe the electrostatic environment of ligands within active sites without perturbing those sites might ultimately allow quantitation of catalytic contributions from preferential electrostatic interactions in the transition state. Such approaches would compare vibrational spectra of enzyme complexes to nonenzymatic standards that relate rate effects to the local electrostatic environment deduced via vibrational spectroscopy.

(31) (a) On the basis of $\beta_{\text{leaving group}} = -1.23$ (see ref 31b), $\log k_1/k_2 = -1.23 \cdot \Delta \text{p}K_{\text{a}} = -1.23 \cdot (4.8 - 17.1) = 15.1$; $\Delta \Delta G = RT \ln(k_1/k_2) = 20.6$ kcal/mol (at 298 K). (b) Kirby, A. J.; Varvoglis, A. G. *J. Am. Chem. Soc.* **1967**, *89*, 415.

(32) Herschlag, D.; Jencks, W. P. *J. Am. Chem. Soc.* **1989**, *111*, 7587.

(33) For review, see: (a) Carey, P. R. *J. Raman Spectrosc.* **1998**, *29*, 7. (b) Callender, R.; Deng, H. *Annu. Rev. Biophys. Biomol. Struct.* **1994**, *23*, 215.

There has been much discussion in enzymology of substrate destabilization and distortion and their possible roles in catalysis. Minimally, the transition state must be preferentially stabilized relative to the ground state, as noted above, and several mechanisms of ground-state destabilization have been suggested.³⁴ A “mild” form of substrate destabilization may be situations in which the enzyme picks out a minor conformer from solution, i.e., a conformation that is not energetically preferred, and stabilizes it at the active site because it is more reactive. This is relatively straightforward when the conformers are close in energy, as is often the case for bond rotations; for example, rotations of amino acid conjugates about the pyridoxal-amine bond results in preferential activation of different bonds.³⁵

More severe forms of substrate destabilization have also been discussed historically, including consideration of enzymes as analogous to the ancient torture device, the “rack”.³⁶ According to this view, the enzyme would stretch the bond to be broken, thereby activating it for reaction. Indeed, there is considerable evidence for bond distortions of enzyme-bound species from

vibrational spectroscopy. Nevertheless, we suggest that these distortions are not necessarily the “intent” of the enzyme in its mission to facilitate catalysis, i.e., that these distortions are not the cause of catalysis, just as we have suggested that the ground-state bond distortions caused by substituents in the alkyl phosphate series are not the cause of the observed rate effects. Rather, we suggest that distortions may be the natural consequence of placing substrates in environments designed to be complementary to transition states. As for the model monosubstituted phosphates, the interactions from the surrounding environment are the cause of both the ground-state physical distortions and the transition-state energetic stabilization. The extent of distortion in the ground state will reflect the stiffness of the bonds in question and the nature of the surroundings, properties that are of fundamental importance for understanding reactivity and catalysis.

Acknowledgment. This work was supported by the David and Lucille Packard Foundation Fellowship in Science and Engineering (D.H.) and Grants from the National Institutes of Health, GM35183 (R.C.) and GM64798 (D.H.) from the Institute of General Medicine and CA69202 (Z-YZ) from the Cancer Institute. IN-H is an American Heart Association Predoctoral Fellow and gratefully acknowledges the support of and scientific interactions with Doug Rees and members of his laboratory. The authors thank members of the Herschlag laboratory for comments on the manuscript.

JA026481Z

- (34) (a) Jencks, W. P. In *Advances in Enzymology and Related Areas of Molecular Biology*; Meister, A., Ed.; John Wiley & Sons: New York, 1975; p 219. (b) Narlikar, G. J.; Gopalakrishnan, V.; McConnell, T. S.; Usman, N.; Herschlag, D. *Proc. Natl. Acad. Sci. U.S.A.* **1995**, *92*, 3668. (c) Burke, J. R.; Frey, P. A. *Biochemistry* **1993**, *32*, 13220.
- (35) For review, see: Palcic, M. M.; Floss, H. G. In *Vitamin B6 Pyridoxal Phosphate*; Dolphin, D., Poulson, R., Avramovic, O., Eds.; John Wiley & Sons: New York, 1986; p 25.
- (36) Lumry, R. *Adv. Chem. Phys.* **1971**, *21*, 567.
- (37) Jencks, W. P.; Regenstein, J. *Ionization Constants of Acids and Bases*; CRC: Cleveland, OH, 1976; p J187.
- (38) Bourne, N.; Williams, A. J. *Org. Chem.* **1984**, *49*, 1200.
- (39) Zhao, Y.; Zhang, Z.-Y. *Biochemistry* **1996**, *35*, 11797–11804.
- (40) Murto, J. *Acta Chem. Scand.* **1964**, *18*, 1043–1053.
- (41) Solomons, T. W. G. In *Organic Chemistry*; John Wiley & Sons: New York, 1988; p 655.
- (42) Guthrie, J. P.; Cullimore, P. A. *Can. J. Chem.* **1979**, *57*, 797.
- (43) Sauers, C. K.; Jencks, W. P.; Broths, S. J. *J. Am. Chem. Soc.* **1975**, *97*, 5564.

- (44) (a) Trifluoroethyl phosphate was also an outlier in a previous linear free-energy relationship of a series of alkyl phosphates (see ref 44b and references therein). (b) O'Brien, P. J.; Herschlag, D. *Biochemistry* **2002**, *41*, 3207.